引用格式：GE Yanqing, LIU Yuqi, LU Chunhui, et al. Third-order Nonlinear Optical Properties of Vertically Aligned SnS_2 Films (Invited)[J]. Acta Photonica Sinica, 2022, 51(10):1019002
葛燕青,刘玉琪,卢春辉,等. 直立生长的SnS_2薄膜的三阶非线性光学性质研究(特邀)[J].光子学报,2022,51(10):1019002

直立生长的SnS_2薄膜的三阶非线性光学性质研究（特邀）

葛燕青,刘玉琪,卢春辉,罗铭威,韩涛涛,周译玄,徐新龙
(西北大学 物理学院 光子学与光子技术研究所, 西安 710127)

摘　要：采用化学气相沉积法制备了直立生长的SnS_2(V-SnS_2)薄膜,并使用自主搭建的Z扫描系统研究了V-SnS_2的三阶非线性光学响应。结果表明,由于S空位的存在使得V-SnS_2薄膜表现出明显的饱和吸收响应,且非线性吸收系数(β)随着泵浦功率的增加而减少。分析发现,其β的最大值为6 cm/GW,调制深度(ΔM)为50%。同时,通过闭口Z扫描技术测量发现V-SnS_2薄膜的n_2比Si和GaAs大一个数量级,且n_2随着泵浦功率的增加而减少,基于自由载流子的非线性理论分析表明这与材料中的自由载流子和束缚电子密切相关。本文研究证明V-SnS_2在全光开关、激光调Q等非线性光电子器件的设计与制造方面有潜在的应用。

关键词：SnS_2;非线性吸收;非线性折射;泵浦功率依赖;Z扫描
中图分类号：O437　　**文献标识码**：A　　**doi**：10.3788/gzxb20225110.1019002

0　引言

近年来,二维(2D)层状金属硫族化合物优异的物理化学性质引起了研究者们的广泛关注。高的载流子迁移率、强的光和物质之间的相互作用以及层数依赖的带隙等电学和光学性质,使其在光电探测器、太阳能电池、光调制器和可饱和吸收器等领域得到快速发展[1-4]。SnS_2作为一种新兴的2D窄带隙半导体材料(2.0～2.6 eV)[5],具有CDI_2型晶体结构,层间弱的范德瓦尔斯力导致了SnS_2的2D特征[6]。

在线性光电特性研究中,SnS_2表现出高的光吸收系数(α_0～10^5～10^6 cm^{-1})[7]、高载流子迁移率(230 cm^2 V^{-1} S^{-1})[8]和大的开关比(>10^6)[8]等优异光电特性。然而,对于SnS_2的非线性光学性质的探索依然处于起步阶段。目前研究者们主要利用旋涂法、化学气相沉积法和液相剥离法制备出了2D SnS_2薄膜并对其非线性吸收性质进行初步探索。研究结果表明,在低于材料带隙的激发波长下(λ=1 560 nm, 1 561 nm, 1 040 nm),SnS_2薄膜表现出明显的饱和吸收响应。目前对于这种现象的解释主要归因于材料生长过程中引入的缺陷,并将其应用到激光调Q、锁模等光子器件中[9-11]。相较于2D薄膜材料,直立生长的二维材料有更多的活性位点以及较大的比表面积,因此呈现出更为优异的吸收特性。同样地,在直立生长的MoS_2的三阶光学非线性吸收研究中,证实了大量的边缘活性位点有利于增强其饱和吸收特性[12-14]。然而,目前针对直立生长的SnS_2纳米片的光学非线性以及内部机理的研究亟需进一步探索。

本文采用化学气相沉积法(Chemical Vapor Deposition, CVD)制备了厘米级SnS_2薄膜,并借助扫描电子显微镜(Scanning Electron Microscope, SEM)、X射线光电子能谱(X-ray Photoelectron Spectroscopy, XPS)、拉曼光谱以及线性吸收光谱等表征手段确认了SnS_2薄膜的高质量直立生长。采用自主搭建的开口/闭口(OA/CA)Z扫描系统,在800 nm的激发光下探索了泵浦功率对直立生长的SnS_2薄膜的非线性光学响

基金项目：国家自然科学基金(Nos. 12074311, 11974279)
第一作者：葛燕青(1996—),女,硕士研究生,主要研究方向为二维材料的非线性光学特性。Email: gyq2361657430@163.com
导师(通讯作者)：周译玄(1985—),男,教授,博士,主要研究方向为先进材料光电特性与应用、太赫兹物理。Email: yxzhou@nwu.edu.cn
徐新龙(1976—),男,教授,博士,主要研究方向为超快光学、非线性光学、太赫兹物理。Email: xlxuphy@nwu.edu.cn
收稿日期：2022-06-23;**录用日期**：2022-08-23

应的影响。研究结果表明，在OA Z扫描下，直立生长的SnS_2薄膜表现出明显的饱和吸收，这主要源于S空位缺陷诱导的单光子吸收。并且，其三阶非线性吸收系数(β)的绝对值随着泵浦功率的增加而减少，这主要源于泡利不相容原理。此外，直立生长的SnS_2薄膜的调制深度高达50%，这为高性能非线性器件的设计提供了基础。通过CA Z扫描技术对直立生长的SnS_2薄膜的非线性折射率(n_2)进行测量，其n_2值随着泵浦功率的增加也呈现减小趋势，这主要与材料中的自由载流子和束缚电子有关。基于以上研究发现直立生长的SnS2薄膜在非线性光子学器件的设计与制造方面有潜在的应用前景。

1 V-SnS_2薄膜的制备与表征

1.1 V-SnS_2薄膜的制备

CVD是一种可以实现制备高质量、大面积二维半导体材料的方法，已被广泛应用到半导体工业材料的合成方面。如图1(a)，本文采用独立的双温区CVD系统成功制备了大面积、高质量、直立生长的SnS_2纳米片。SnO (2 mg, 99.9%, Alfa)和S (500 mg, 98%, Aladdin)粉末分别置于管式炉的第一温区和第二温区的中心，提供SnS_2生长过程中所需的Sn和S的来源。选用耐腐蚀，耐高温的1 cm×1 cm的蓝宝石为基底，并将其置于SnO前驱体下游10 cm处。在制备过程中，设置管式炉第一温区和第二温区的温度在15 min内分别升至650℃和200℃，并在此温度下维持5 min完成SnS_2生长，反应过程为：$2SnO + 5S = 2SnS_2 + SO_2$，基底温度约为400℃。实验一直采用30 sccm氩气作为载气，排尽管内氧气防止氧化。根据Bravais定律[15]，由于[100]面具有更高的表面能[16]，SnS_2纳米片更利于直立生长，这与已报道的直立生长SnS_2纳米片结果一致[17]。图1(b)、(c)为直立生长的SnS_2薄膜的表面和截面SEM图。表征结果显示，SnS_2纳米片均匀且密集排列在蓝宝石衬底表面，纳米片平均尺寸约为400 nm，厚度约为750 nm。文中将直立生长的SnS_2定义为V-SnS_2。

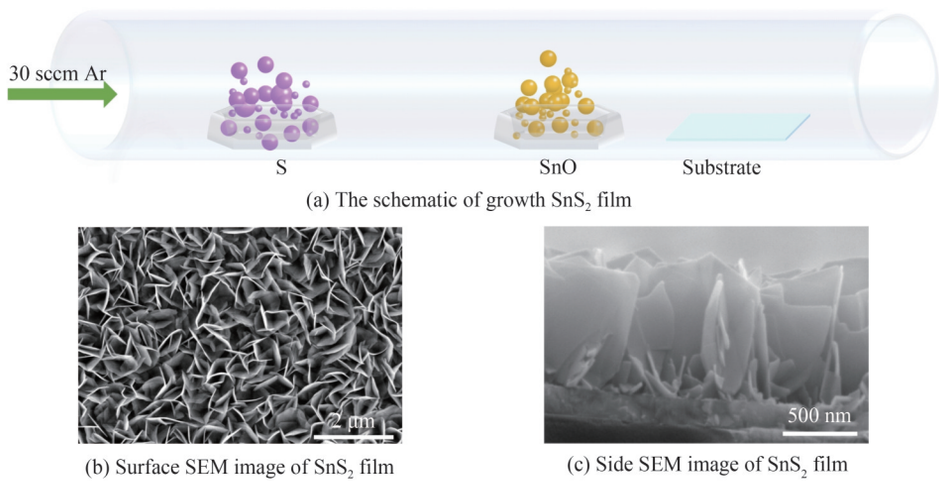

(a) The schematic of growth SnS_2 film

(b) Surface SEM image of SnS_2 film

(c) Side SEM image of SnS_2 film

图1 SnS_2薄膜的制备示意图及表面形貌

Fig. 1 Growth schematic diagram and surface morphology of SnS_2 film

1.2 V-SnS_2薄膜的表征

利用XPS(Thermo Fisher、ESCALAB Xi+)对制备的V-SnS_2的元素含量和化学键信息进行了分析。V-SnS_2的全XPS谱如图2(a)，其中主要元素为Sn、S、O和C，均来自样品和蓝宝石衬底。在图2(b)中可以看出，486.87 eV和495.27 eV处的两个特征峰分别对应于Sn^{4+}的Sn $3d_{5/2}$和Sn $3d_{3/2}$。从图2(c)中可以发现，S 2p对应的结合能峰为161.77 eV和162.97 eV，分别对应于S^{2-}的S $2p_{3/2}$和S $2p_{1/2}$的特征峰，这一结果与先前关于SnS_2的报道一致[18]。此外，通过计算发现Sn/S的值大于2，证明所制备的V-SnS_2薄膜存在大量的S空位。

为进一步表征V-SnS_2薄膜，图2(d)给出了采用配备532 nm激光光源的拉曼光谱仪对V-SnS_2薄膜的测试结果。在313.482 cm^{-1}处的拉曼峰来自于A_{1g}声子模式，与之前报道的SnS_2拉曼光谱一致[19]，进一步证明V-SnS_2样品的成功制备。此外，如图2(e)所示，利用紫外-可见吸收光谱(Ideaoptics R1)表征了V-SnS_2样品的线性吸收特性。V-SnS_2薄膜在800 nm波长处的线性吸收系数约为6.71×10^3 cm^{-1}。

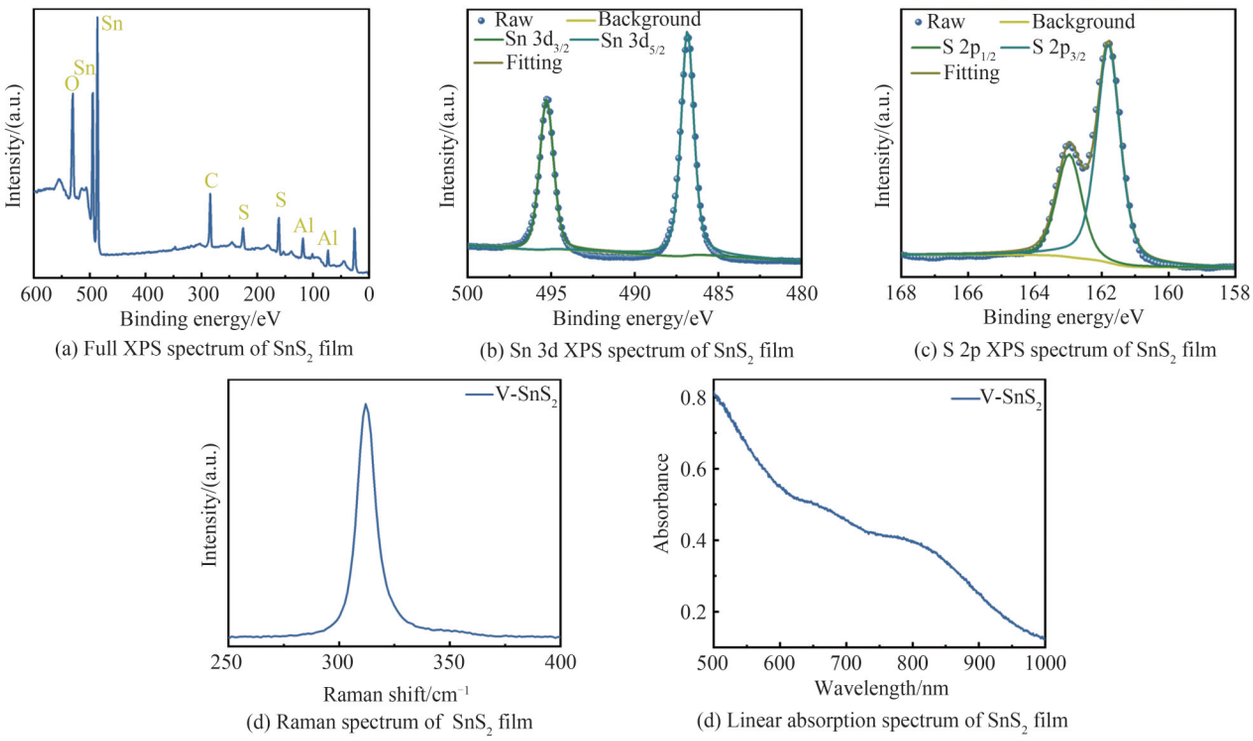

图 2　V-SnS_2薄膜的表征

Fig. 2　Characterization of V-SnS_2 film

2　结果与讨论

2.1　实验设备

采用自主搭建的开孔和闭孔Z扫描系统探索了V-SnS_2薄膜的非线性吸收和折射性质。实验所使用的激光光源为光谱物理公司的Ti:蓝宝石飞秒激光器，其中心波长为800 nm，重复频率为1 kHz，脉冲宽度为35 fs，最大输出功率为5 W。激光强度由衰减器、$\lambda/2$波片和Glan-Taylor棱镜衰减。OA/CA Z扫描信号可以通过一个光阑实现调节。获得的透射强度（T）与位置（Z）的信号，经由硅探测器（Thorlabs：PDA100A（－EC））采集和检测，最终由锁相放大器放大并降低噪声信号的干扰。

2.2　V-SnS_2薄膜的非线性光学吸收

为探究泵浦强度对V-SnS_2薄膜的非线性吸收过程的影响，采用OA Z扫描技术在600～1 000 GW/cm^2下测量了V-SnS_2薄膜的T-Z的关系。此外，在1 200 GW/cm^2处测量了蓝宝石基底的非线性响应，结果显示并未出现明显的非线性响应，这对于研究SnS_2材料的非线性性质没有影响。图3（a）为在泵浦强度为600～1 000 GW/cm^2的范围内V-SnS_2薄膜的T-Z曲线，在Z=0处呈现峰的形状，表明V-SnS_2薄膜在不同泵浦强度下（600～1 000 GW/cm^2）均表现出明显的饱和吸收（SA）特性。

文献调研发现SnS_2薄膜的带隙为2.0～2.6 eV[5]，远远大于光子能量（1.55 eV；800 nm）。因此，在V-SnS_2薄膜中不能发生单光子吸收。根据之前的XPS表征，推断V-SnS_2薄膜的SA可以归因于S空位引起的缺陷状态。因此，V-SnS_2薄膜SA的带间跃迁过程可以简化为图3（c）。在激发光子能量为1.55 eV下，SnS_2中价带的电子无法借助单光子吸收过程，直接跃迁到导带。基于上述分析发现，由于S空位缺陷的存在，会在SnS_2的导带和价带之间引入缺陷态，价带顶部的电子可以借助缺陷态，实现导带底部的跃迁，从而表现出SA现象[8; 10]，这与S空位缺陷的MoS_2和ReS_2出现SA结果一致[12; 20]。

样品的线性吸收和非线性吸收关系可以表示为$\alpha(I)=\alpha_0+\beta I$，$\alpha_0$代表线性吸收系数，$\beta$是非线性吸收系数。为了提取所制备的V-$SnS_2$薄膜的$\beta$值，图3（a）中的$Z$扫描实验数据可以用式（1）拟合[21]

$$T_{\mathrm{OA}}=\sum_{m=0}^{\infty}\frac{\left[-\beta I_0 L_{\mathrm{eff}}/\left(1+Z^2/Z_0^2\right)\right]^m}{(m+1)^{3/2}}\qquad (m=1,2,3) \tag{1}$$

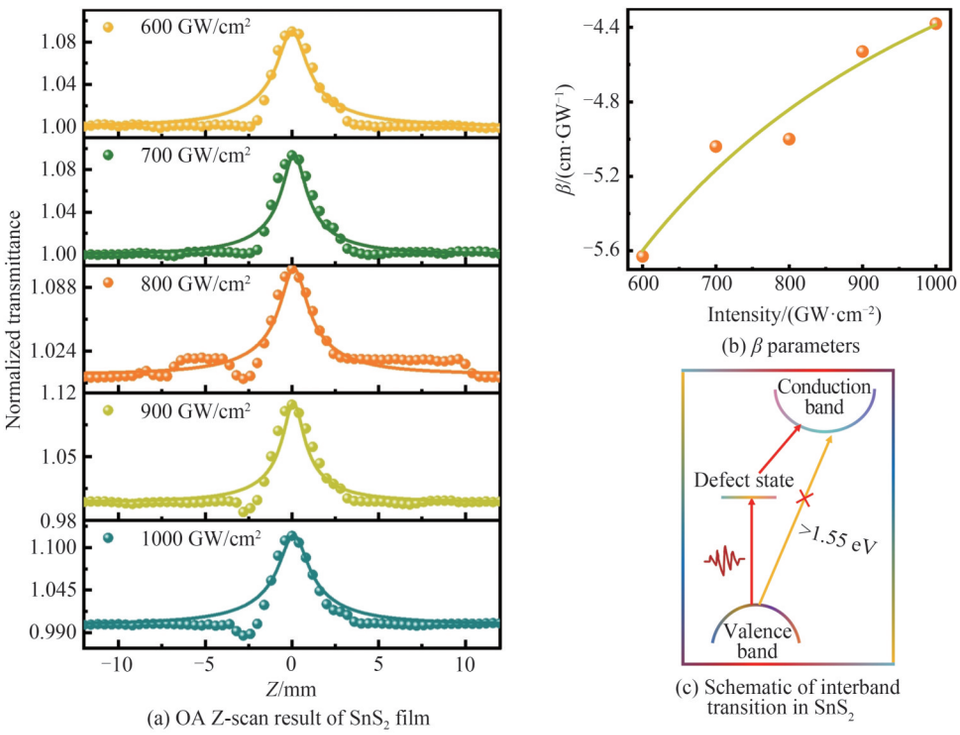

图 3 不同泵浦功率下 V-SnS_2薄膜的 OA Z 扫描结果及 SA 的带间跃迁图

Fig. 3 The OA Z-scan results of V-SnS_2 film at different pump intensities and the schematic of interband transition

式中，$L_{\mathrm{eff}}=\left(1-\mathrm{e}^{-\alpha_0 L}\right)/\alpha_0$是 V-$SnS_2$薄膜的有效厚度，$I_0$是样品在焦点处的泵浦光强。在泵浦光强为 600 GW/cm^2和 1000 GW/cm^2时，V-SnS_2薄膜的β值分别为－6.0 cm/GW 和－4.64 cm/GW，大于 V-WS_2（－0.63 cm/GW）[22]、黑鳞纳米片（-7.21×10^{-3} cm/GW）[23]和MoS_2纳米片（-3×10^{-4} cm/GW）[24]等。在图 3(b)中可以清楚地发现，β的绝对值随着泵浦强度的增加而减小，这种与泵浦强度相关的非线性光学吸收现象可以通过泡利不相容原理来解释，即一个量子系统内，同一个量子态不能同时被两个或两个以上的费米子（比如电子）占据[25]。同时，通过计算发现 V-SnS_2薄膜的调制深度（$\Delta M=\alpha_0 L$）约为 50%，远远高于之前报道的 V-SnS_2（11.7%）[19]、MoS_2（27%）[26]和$ReSe_2$（27%）[27]。这主要源于直立的纳米结构更利于光子的捕获，因此表现出更高的非线性吸收和调制深度，使 V-SnS_2纳米片在调 Q 和锁模等方面具有更好的前景。

2.3 V-SnS_2薄膜的非线性光学折射

利用 CA Z 扫描技术探索了 V-SnS_2薄膜的非线性折射响应与泵浦强度的关系。如图 4(a)～(e)所示，在泵浦强度为 600～1 000 GW/cm^2的范围内 V-SnS_2薄膜的 CA 曲线显示出“谷-峰”结构，这是典型的自聚焦现象。实验结果可由式(2)拟合[28]

$$T_{\mathrm{CA}}=1+\frac{4kL_{\mathrm{eff}}n_2I_0z}{\left(1+Z^2/Z_0^2\right)\left(9+Z^2/Z_0^2\right)} \tag{2}$$

式中，$k=2\pi/\lambda$，n_2表示非线性折射率。这里需要将 CA Z 扫描结果除以 OA 结果，以消除 SA 对 V-SnS_2薄膜非线性折射的影响。用式(2)拟合 CA 实验数据，得到了n_2对 V-SnS_2薄膜的泵浦强度依赖关系，如图 4(f)。对于 V-SnS_2薄膜，n_2值随泵浦强度增加呈下降趋势，这可以用幂函数拟合$\beta=A+B\times(1/I)$。此外，V-SnS_2薄膜的n_2比传统的 Si 和 GaAs 半导体大一个数量级[29]。同样地，相较于SnS_2薄膜的非线性折射率（$n_2=1.1\times10^{-17}$ m^2/W）[30]，直立的SnS_2纳米片可以实现更高的非线性折射率（$n_2=1.89\times10^{-17}$ m^2/W），这与直立MoS_2非线性研究结果一致[12]。这种边缘接触光场相比于面接触光场产生更强的非线性特性，可以归因于直立的二维材料具有大量的边缘活性位点[31]。

V-SnS_2薄膜的泵浦强度依赖的非线性折射率与自由载流子和束缚电子的关系可以表示为$n_2=n_2^*+\sigma_\gamma N(t)/I$，其中$n_2^*$为束缚电荷引起的非线性折射率系数，$\sigma_\gamma$代表自由载流子折射系数，$N(t)$是由线性和非线

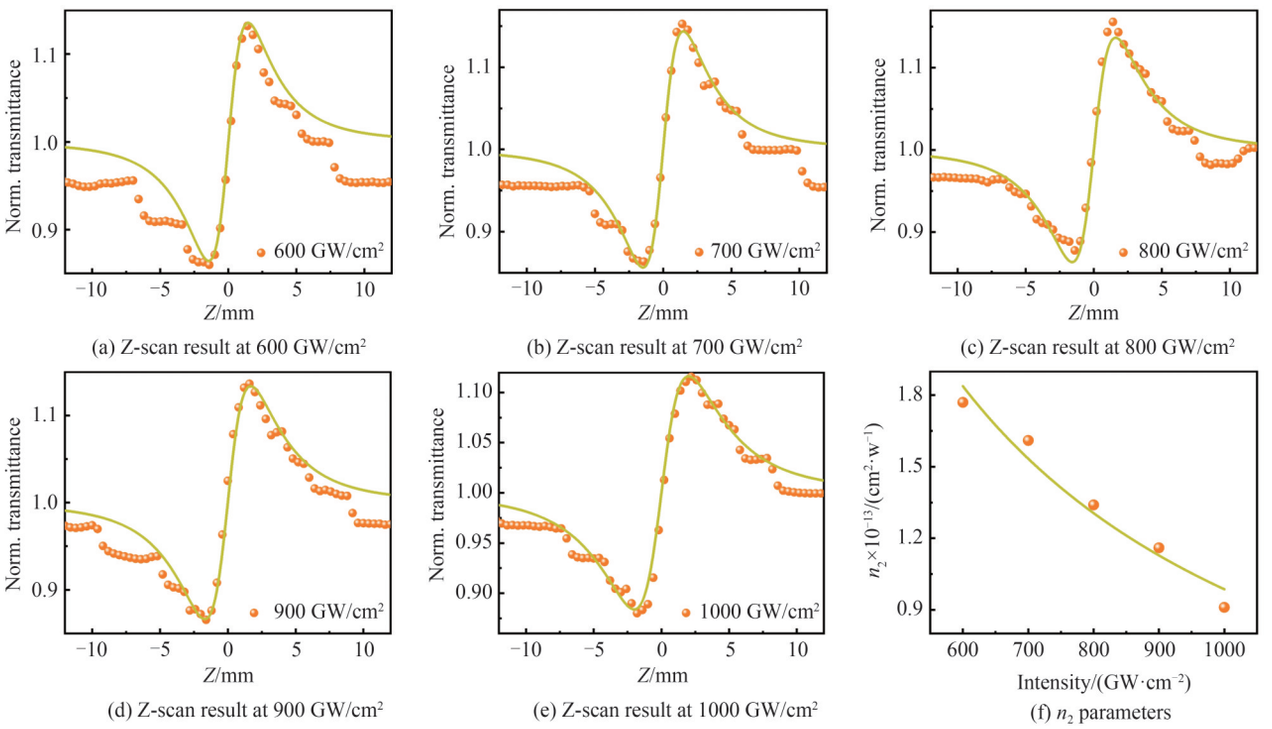

图 4　不同泵浦功率下V-SnS_2薄膜的CA Z扫描结果

Fig. 4　The CA Z-scan results of V-SnS_2 film at different pump intensities

性吸收结合产生的光激发载流子密度[32]。因此，当V-SnS_2薄膜的泵浦强度达到600 GW/cm²时，价带中的电子会发生单光子吸收，从而减弱了束缚电子对非线性的影响。同时，自由载流子密度保持相对稳定，因此非线性折射率随入射光强的增加而减小[33]。

3　结论

本文通过CVD法制备了V-SnS_2薄膜，利用OA/CA Z扫描技术系统地研究了泵浦功率对其非线性响应的影响。结果表明，V-SnS_2薄膜表现出明显的SA响应，且其β的绝对值随着泵浦功率的增加而减小，主要源自于泡利不相容原理。SA响应主要归结于S空位缺陷辅助的单光子吸收。V-SnS_2薄膜的β的最大值和调制深度分别为6 cm/GW和50%。与此同时，测量了V-SnS_2薄膜的n_2，发现其n_2值也随着泵浦功率的增加而减小，基于自由载流子的非线性理论分析表明其与材料中的自由载流子和束缚电子有关。此外，V-SnS_2薄膜的n_2都比Si和GaAs大一个数量级。研究结果证明V-SnS_2薄膜在激光调Q和全光开关等非线性光电子学器件研发领域具有潜在应用前景。

参考文献

[1] LI Xiaobo, CUI Fangfang, FENG Qingliang, et al. Controlled growth of large-area anisotropic ReS_2 atomic layer and its photodetector application[J]. Nanoscale, 2016, 8(45): 18956-18962.

[2] LU Chunhui, LUO Mingwei, GE Yanqing, et al. Layer-dependent nonlinear optical properties of WS_2, MoS_2, and Bi_2S_3 films synthesized by chemical vapor deposition[J]. ACS Applied Materials & Interfaces, 2022, 14(1): 2390-2400.

[3] ZHAO Mei, ZHANG Wenting, LIU Manman, et al. Interlayer coupling in anisotropic/isotropic van der Waals heterostructures of ReS_2 and MoS_2 monolayers[J]. Nano Research, 2016, 9(12): 3772-3780.

[4] MAO Dong, WANG Yadong, MA Chaojie, et al. WS_2 mode-locked ultrafast fiber laser[J]. Scientific Reports, 2015, 5: 7965.

[5] YE Gonglan, GONG Yongji, LEI Sidong, et al. Synthesis of large-scale atomic-layer SnS_2 through chemical vapor deposition[J]. Nano Research, 2017, 10(7): 2386-2394.

[6] LI Guoqiang, WU Chi, ZHANG Shuaiyi, et al. Passively Q-switched Er:YAG laser at 1645 nm with SnS_2 as a novel saturable absorber[J]. Optik, 2019, 183: 163-167.

[7] WANG Bing, ZHONG Shipeng, ZHANG Zhibin, et al. Broadband photodetectors based on 2D group IVA metal chalcogenides semiconductors[J]. Applied Materials Today, 2019, 15: 115-138.

[8] HU Yi, CHEN Tao, WANG Xiaoqi, et al. Controlled growth and photoconductive properties of hexagonal SnS_2 nanoflakes with mesa-shaped atomic steps[J]. Nano Research, 2017, 10(4): 1434-1447.
[9] LI Shi, YIN Yu, OUYANG Qiuyun, et al. Dissipative soliton generation in Er-doped fibre laser using SnS_2 as a saturable absorber[J]. Applied Physics Express, 2019, 12(10): 102008.
[10] LIU Wenjun, LIU Mengli, WANG Xiaoting, et al. Thickness-dependent ultrafast photonics of SnS_2 nanolayers for optimizing fiber lasers[J]. ACS Applied Nano Materials, 2019, 2(5): 2697-2705.
[11] WANG Rui, ZHANG Luwei, SUN Tao, et al. Preparation and characteristics of SnS_2 saturable absorber and its application in passively Q-switched Nd:YAG/Cr^{4+}:YAG laser[J]. Optik, 2020, 212: 164712.
[12] ZHANG Xiaoyan, ZHANG Saifeng, CHEN Bohua, et al. Direct synthesis of large-scale hierarchical MoS_2 films nanostructured with orthogonally oriented vertically and horizontally aligned layers[J]. Nanoscale, 2016, 8(1): 431-439.
[13] WEI Rongfei, TIAN xiangling, HU Zhongliang, et al. Vertically standing layered MoS_2 nanosheets on TiO_2 nanofibers for enhanced nonlinear optical property[J]. Optics Express, 2016, 24(22): 25337-25344.
[14] RAHMATI B, GHAYEB-ZAMHARIR S, KARIMZADEH R, et al. Nonlinear optical properties of vertically-aligned MoS_2 nanosheets[J]. Journal of Electronic Materials, 2021, 50(6): 3645-3651.
[15] MA Xinghua, CHO Kihyun, SUNG Yunmo. Growth mechanism of vertically aligned SnSe nanosheets via physical vapour deposition[J]. CrystEngComm, 2014, 16(23): 5080-5086.
[16] LI Mengyi, LIU Enzuo, HU Huilin, et al. Surfactant-free synthesis of single crystalline SnS_2 and effect of surface atomic structure on the photocatalytic property[J]. International Journal of Photoenergy, 2014, 2014: 1-7.
[17] LIU Guangbo, LI Zhonghua, HASAN Tawfique, et al. Vertically aligned two-dimensional SnS_2 nanosheets with a strong photon capturing capability for efficient photoelectrochemical water splitting[J]. Journal of Materials Chemistry A, 2017, 5(5): 1989-1995.
[18] ZHANG Yiqiong, MA Zhaoling, LIU Dongdong, et al. p-Type SnO thin layers on n-type SnS_2 nanosheets with enriched surface defects and embedded charge transfer for lithium ion batteries[J]. Journal of Materials Chemistry A, 2017, 5(2): 512-518.
[19] HE Junshan, LOU Yajun, LI Yonghui, et al. Preparation of vertically aligned two-dimensional SnS_2 nanosheet film with strong saturable absorption to femtosecond laser[J]. Journal of Physics D: Applied Physics, 2019, 52(16): 165101.
[20] MAO Dong, CUI Xiaoqi, GAN Xuetao, et al. Passively Q-switched and mode-locked fiber laser based on an ReS_2 saturable absorber[J]. IEEE Journal of Selected Topics in Quantum Electronics, 2018, 24(3): 1-6.
[21] QUAN Chenjing, LU Chunhui, HE Chuan, et al. Band alignment of $MoTe_2$/MoS_2 nanocomposite films for enhanced nonlinear optical performance[J]. Advanced Materials Interfaces, 2019, 6(5): 1801733.
[22] FU Xiuli, QIAN Jingwen, QIAO Xiaofen, et al. Nonlinear saturable absorption of vertically stood WS_2 nanoplates[J]. Optics Letters, 2014, 39(22): 6450-6453.
[23] XU Yanhua, JIANG Xiaofang, GE Yanqi, et al. Size-dependent nonlinear optical properties of black phosphorus nanosheets and their applications in ultrafast photonics[J]. Journal of Materials Chemistry C, 2017, 5(12): 3007-3013.
[24] ZHOU Kaige, ZHAO Min, CHANG Mengjie, et al. Size-dependent nonlinear optical properties of atomically thin transition metal dichalcogenide nanosheets[J]. Small, 2015, 11(6): 694-701.
[25] ZHANG Baitao, LIU Jun, WANG Cong, et al. Recent progress in 2D material-based saturable absorbers for all solid-state pulsed bulk lasers[J]. Laser & Photonics Reviews, 2019, 14(2): 1900240.
[26] WANG Shuxian, YU Haohai, ZHANG Huaijin, et al. Broadband few-layer MoS_2 saturable absorbers[J]. Advanced Materials, 2014, 26(21): 3538-3544.
[27] WANG Na, LU Baole, QI Xinyuan, et al. Passively Q-switched ytterbium-doped fiber laser with $ReSe_2$ saturable absorber[J]. Optics and Laser Technology, 2019, 116: 300-304.
[28] LIU Dong, LIU Junting, ZHANG Kangning, et al. Giant nonlinear optical response of lead-free all-inorganic $CsSnBr_3$ nanoplates[J]. Journal of Physical Chemistry C, 2021, 125(1): 803-811.
[29] DINU M, QUOCHI F, GARCIA H. Third-order nonlinearities in silicon at telecom wavelengths[J]. Applied Physics Letters, 2003, 82(18): 2954-2956.
[30] PETRIS A, GHEORGHE P S, VLAD V I, et al. Ultrafast third-order optical nonlinearity in SnS_2 layered compound for photonic applications[J]. Optical Materials, 2018, 76: 69-74.
[31] YIN X, YE Z, CHENET D A, et al. Edge nonlinear optics on a MoS_2 atomic monolayer[J]. Science, 2014, 344(6183): 488-490.
[32] CHEN Runze, ZHENG Xin, ZHANG Yangwei, et al. Z-scan measurement of nonlinear optical properties of BiOCl nanosheets[J]. Applied Optics, 2015, 54(21): 6592-6597.
[33] LU Shunbin, ZHAO Chujun, ZOU Yanhong, et al. Third order nonlinear optical property of Bi_2Se_3[J]. Optics Express, 2013, 21(2): 2072-2082.

Third-order Nonlinear Optical Properties of Vertically Aligned SnS_2 Films (Invited)

GE Yanqing, LIU Yuqi, LU Chunhui, LUO Mingwei, HAN Taotao, ZHOU Yixuan, XU Xinlong

(*Institute of Photonics & Photon-technology, School of Physics, Northwest University, Xi'an* 710127, *China*)

Abstract: Two-dimensional (2D) layered metal dichalcogenides have attracted extensive attention due to their unique physicochemical properties, such as high carrier mobility, strong light-matter interaction and tunable band gap. Tin disulfide (SnS_2), as an emerging 2D layered metal dichalcogenides with a narrow band gap (2.0～2.6 eV), has a CDI_2 type crystal structure and the layered structure is formed by a stack of sandwiched S-Sn-S planes connected by van der Waals force. Furthermore, SnS_2 is non-toxic, low-cost, and storage abundant, which meets the need of industrial production of electronic and optoelectronic devices. It also exhibits excellent photoelectric responses such as high absorption coefficient ($\alpha_0 \sim 10^5 \sim 10^6$ cm^{-1}), large on/off ratio ($>10^6$), high carrier mobility (230 cm^2 $V^{-1}S^{-1}$), and so on, which ensures its rapid development in photoelectric applications such as photodetectors, solar cells and photocatalysis. However, so far, research on the nonlinear optical properties of SnS_2 films is still in infancy. In the early stage, SnS_2 was prepared by liquid phase exfoliation technique to firstly explore its nonlinear optical properties. The SnS_2 films always show saturable absorption under the lower photon energy than band gap. This saturable absorption can be explained by some surface defects, coming from the growth process. As such, many novel 2D semiconductors such as WS_2 and MoS_2 with S vacancy defect also have been demonstrated and successfully applied into mode-locked, Q-switched, and other photonic devices. The defects can capture excitons, electrons, and holes to modulate nonlinear absorption. Thus, it is necessary to confirm the defect type and then systematically analyze the nonlinear optical response of SnS_2 films. Compared with horizontally aligned 2D film, vertically aligned materials have larger specific surface area and exposed edge sites, thus resulting in higher light absorption characteristics. Furthermore, the active edges of MoS_2 have shown a strong resonant nonlinear optical susceptibility and the vertically aligned WS_2 shows higher modulation performance. Thus, it is crucial and meaningful to prepare vertically aligned SnS_2 layers, which are promising to exhibit an excellent nonlinear optical property. Recently, vertically aligned SnS_2 layers have been successfully synthesized by hydrothermal method. However, impurity and surface roughness would provide a large contribution for the nonlinear scattering and result in sophistication in the mechanism analysis of nonlinear optical response. Herein, it is noteworthy that the controllable synthesis of vertically aligned SnS_2 layers is also the key to study the nonlinear optical response. Compared with liquid phase exfoliation method and hydrothermal method, Chemical Vapor Deposition (CVD) has been demonstrated as an effective and general method to prepare 2D film in large-area. In this paper, large-area SnS_2 films are prepared by CVD method using SnO and S powders as precursors and c-plane sapphire is selected as target substrate. The SnS_2 nanosheets are uniform and well-aligned on the c-plane sapphire substrate characterized by scanning electron microscopy. The average width of nanosheets is approximately 400 nm and the thickness of nanosheets is about 750 nm. X-ray photoelectron spectroscopy and Raman spectroscopy confirm the successful preparation of high-quality vertically aligned SnS_2 film. The effect of pump power on the nonlinear optical response of vertically aligned SnS_2 film is investigated at 800 nm by using open/close aperture (OA/CA) Z-scan technique. The results show that the vertically aligned SnS_2 film exhibits an obvious saturable absorption. This can be due to the S-vacancy defect single induced photon absorption and the corresponding defects are characterized by X-ray photoelectron spectroscopy. The calculated results show that the third-order nonlinear absorption coefficient (β) of vertically aligned SnS_2 film is 1-2 orders of magnitude larger than that of previously reported 2D nanosheets, and the absolute value of β decreases with the pump intensity, which is mainly contributed to the Pauli blocking effect. With the increase of incident laser intensity, electrons in the valence band are continuously excited to the defect state and transmitted to the conduction band until electrons and holes occupy nearly half of the photon energy in the valence band and conduction band. Due to Pauli blocking effect, the interband transitions are blocked and the saturable absorption response takes place. At this time, the relationship

between total absorption can be expressed as $\alpha(I)=\alpha_0/(1+I/I_S)$. More importantly, the modulation depth of vertically aligned SnS_2 is up to 50%, which provides a reference for designing high-performance nonlinear photonic devices. In addition, the nonlinear refractive index (n_2) of SnS_2 film grown vertically is also measured, and the values of n_2 also decrease with the pump intensity, which is mainly related to the free carriers and bound electrons of the material. Meanwhile, the n_2 for vertically aligned SnS_2 film is comparable to previously reported 2D nanosheets, such as WS_2, WSe_2, MoS_2, $MoSe_2$, and $MoTe_2$. Based on the above-analyzed results, we find that vertically aligned SnS_2 film has a great potential in the design and manufacture of nonlinear photonic devices.

Key words: SnS_2; Nonlinear absorption; Nonlinear refraction; Pump intensity dependence; Z-scan

OCIS Codes: 190.4400; 230.0250; 160.4330

Foundation item: National Natural Science Foundation of China (Nos. 12074311, 11974279)